Water Practice & Technology

IWA PUBLISHING

Water Practice & Technology Vol 17 No 3, 784 doi: 10.2166/wpt.2022.018

Pristine and activated bentonite for toxic metal removal from wastewater

Tope B. Ibigbami[a], Adedapo O. Adeola[b,*], David B. Olawade[c], Odunayo T. Ore[d], Babatunde O. Isaac[e] and Alabi A. Sunkanmi[f]

[a] Environment and Air Quality Assessment Department, Healthy Life for All Foundation, University College Hospital, Ibadan, Oyo State, Nigeria
[b] Department of Chemical Sciences, Adekunle Ajasin University, 001 Akungba-Akoko, Ondo State, Nigeria
[c] Department of Environmental Health Sciences, University of Ibadan, Ibadan, Oyo State, Nigeria
[d] Department of Chemistry, Obafemi Awolowo University, Ile-Ife, Osun State, Nigeria
[e] Integrated Engineering and Environmental Department, Geoterrain Nigeria Limited, Lekki, Lagos State, Nigeria
[f] Marcoe Aquafit Technical Services, Agege, Lagos State, Nigeria
*Corresponding author. E-mail: adedapo.adeola@aaua.edu.ng

AOA, 0000-0002-7011-2396; OTO, 0000-0002-5529-1509

ABSTRACT

Natural bentonite clay (NBC) was activated using nitric acid (HNO_3). Characterization techniques including FTIR, SEM, XRD and BET were employed to examine the morphology of NBC and ABC (activated bentonite clay) sorbents. Comparative application of ABC and NBC to remove heavy metals (Fe^{2+}, Zn^{2+}, Ni^{2+}) from pharmaceutical effluents was investigated under various experimental conditions. The maximum proportional removal by ABC was 88.90, 81.80 and 75.50% at pH 8, and 63.90, 59.60, 58.70% at pH 10 for NBC, both for $Zn^{2+,}$ Fe^{2+} and Ni^{2+} respectively. The Freundlich multilayer adsorption model and pseudo-second-order kinetics best fit the experimental data, suggesting the formation of multiple adsorption layers via strong ionic and electrostatic interactions. Heavy metals adsorption is more favorable with ABC than NBC, due to the availability of more sorption sites and a larger specific surface. The thermodynamic parameters ($\Delta H°$, $\Delta S°$, and $\Delta G°$) revealed that the adsorption is endothermic and spontaneous in nature for both ABC and NBC.

Key words: adsorption, bentonite clay, heavy metals, kinetics, thermodynamics

HIGHLIGHTS

- Acid activation of bentonite clay using nitric acid was achieved in this study.
- Enhanced morphology and physicochemical properties of pristine bentonite was observed.
- Removal efficiency > 85% of recalcitrant heavy metals was obtained using modified bentonite.
- Pre-oxidation of contaminated water using H_2O_2 enhanced clean-up efficiency.
- Adsorption process was spontaneous, endothermic, and best described by multilayer sorption.

GRAPHICAL ABSTRACT

1. INTRODUCTION

Metal pollution of surface waters is often due to indiscriminate discharge of the metals or wastewater containing the metals into watercourses (Ahmetović *et al.* 2019). Heavy metals are hazardous to humans and aquatic fauna due to their poor degradability, biomagnification tendencies, and the toxicity of high concentrations (Ore & Adeola 2021). These hazards necessitate legislation against the direct discharge of heavy metals into the environment. Remedial alternatives for heavy metal removal from aqueous solution include adsorption, coagulation, flocculation, electrochemical removal, ion exchange, bioremediation, membrane filtration, chemical precipitation, etc (Burakov *et al.* 2018; Zhao *et al.* 2020). However, the limitations associated with most of them include the costs of handling sludge/secondary pollutants, sensitive operating conditions, low efficiency, toxic sludge generation, high energy consumption, and incomplete removal (Kanamarlapudi *et al.* 2018; Ore & Adeola 2021).

Adsorption has demonstrated high efficiency in water treatment against many contaminants, particularly heavy metals (Abu-Danso *et al.* 2020). Adsorption techniques can be scaled up, whilst avoiding toxic by-products/metabolite production during treatment, a common problem with photocatalytic- and bio-degradation. The ease of recovery, regeneration, and reusability of many adsorbents also presents a sustainable and cost-effective approach to pollution remediation (Adebiyi *et al.* 2021). Clay minerals, which are naturally abundant, have has a significant historical impact on civilization (Ismadji *et al.* 2015). Bentonite is a 2:1 clay mineral composed primarily of montmorillonite (Maged *et al.* 2020). The distinct physicochemical properties of bentonite – for example, low permeability, low cost, strong absorptive affinity with inorganic and organic substances, large specific surface, small particle size, high porosity, and high cation exchange capacity – make it an effective adsorbent of different kinds of pollutants (Uddin 2017).

Chemical activation, using H_2SO_4, NaCl, and phosphoric acid, has been used to increase the specific surface of natural bentonite. However, there are few reports of the use of nitric acid for such activation. Bentonite was activated with nitric acid in this study, which was then subject to detailed characterization. Adsorption of Fe^{2+}, Zn^{2+}, and Ni^{2+} from wastewater from the pharmaceutical industry was studied under various process conditions. The interaction mechanisms between heavy metals and unmodified and/or activated bentonite were also investigated, using established isotherm and kinetic models.

2. MATERIALS AND METHODS

2.1. Clay sample collection

Fresh bentonite for use in this study was collected from the Federal Institute of Industrial Research (FIIRO), Oshodi, Lagos State, Nigeria. The 750 g sample was oven-dried (70 ± 1 °C), crushed, ground, and sieved to fine powder (<150 μm).

2.2. Pharmaceutical industrial effluents

Pharmaceutical industry wastewater was collected in Ibadan, Nigeria, before discharge to a nearby stream. Sampling bottles were washed with dilute hydrochloric acid, rinsed with de-ionized water and dried for 2 hours at 120 ± 3 °C. At the sampling location they were rinsed with the effluent three times prior to sample collection. The bottles were transported in a cooler box to the laboratory for treatment and analysis (Ibigbami *et al.* 2016). Sample pH and temperature were taken at the time of collection using a pocket-pen type of pH meter.

2.3. Chemicals and equipment

The analytical grade nitric acid (HNO_3) used as activating agent for the bentonite; sodium hydroxide (NaOH), hydrogen peroxide 30% w/w (H_2O_2), sodium chloride (NaCl), sodium acetate (Na-Ac), and acetic acid (98% purity) were purchased from Sigma-Aldrich (Germany).

Sorbent preparation was carried out using a high-temperature resistance furnace (SXL-1200, Zhengzhou Honglang), magnetic stirrer (JJ-4, Changzhou Guowang), microwave oven (MG-5021, Seoul, South Korea), shaking water bath (DK-98-1, Shanghai, China), and centrifuge (TGL-16G, Shanghai, China). Instruments used for sorbent characterization included; UV spectrophotometer (200–1,000 nm, UV-2350, Unico), scanning electron microscope (JSM-6360LV, JEOL), X-ray powder diffractometer (Angle range: 5–120°, Bruker AXS GmbH, Karlsruhe, Germany), and infrared spectrometer (PE-680, PerkinElmer).

2.4. Adsorbent preparation

2.4.1. Bentonite pre-treatment

The natural bentonite (NBC) was treated to remove calcite, other carbonates, and organic matter by washing with Milli-Q water. After drying, 25 g were added to 400 mL of 0.1 N Na-Ac solution containing acetic acid to regulate the pH ≈ 5.0. The suspension was stirred for 12 hours at 70 ± 1 °C. Stirring was continued overnight at ambient temperature with gradual addition of 100 mL of H_2O_2, before the suspension was centrifuged and washed three times with 0.01 N NaCl solution and Milli-Q water, consecutively. The residue was then dried at 105 ± 1 °C for 24 hours in a laboratory oven. The resulting NBC was pulverized, sieved (100 μm mesh-size) and stored in a desiccator.

2.4.2. Bentonite activation

NBC was introduced to 2M HNO_3 at a mass:volume ratio of 1:2. The suspension was agitated in a thermostat-controlled water bath at 70 ± 1 °C for 4 hours, after which the residue was washed several times with deionized water. The viscous residue was oven-dried at 60 °C for 24 hours, and the resultant ABC pulverized and sieved (100 μm mesh size).

2.5. Sorbent characterization

The morphological distinctions between NBC and ABC were established by analysis using the Brunauer-Emmet-Teller (BET) method, Fourier transform infrared spectroscopy (FTIR), scanning electron microscopy (SEM) and X-ray diffraction (XRD). The specific surface and pore distribution of the powdered samples were determined by comparing N_2 gas adsorption onto the surface of the solid with the amount of gas required to form a monolayer on the adsorbent surface. The cation exchange capacity (CEC) of the samples was determined using the copper bis-ethylenediamine complex method (Bergaya & Vayer 1997).

2.6. Wastewater sample digestion and treatment

Wet digestion was employed to remove organics from the wastewater and release metals bound to organic matter (Kinuthia *et al.* 2020). Fe, Zn and Ni adsorption from the wastewater using NBC and ABC was investigated in 40 mL amber vials. The roles of contact time, adsorbent dosage, solution pH, H_2O_2 oxidation and temperature on treatment efficiency were examined. The data obtained were used to calculate the equilibrium metal uptake capacity using Equation (1):

$$q_e = \frac{(C_0 - C_e)V_0}{S_m} \tag{1}$$

$$\text{Removal efficiency (\%)} = \frac{(C_0 - C_e)}{C_0} \times 100 \tag{2}$$

where C_0 is the initial concentration of Fe, Zn or Ni (100–500 mg/L); C_e the equilibrium concentration of the ions concerned (mg/L); q_e amount of heavy metal ions adsorbed per unit weight of adsorbent (mg/g); V the solution volume (mL); and m the adsorbent dose (mg).

3. RESULTS AND DISCUSSION

3.1. Sorbent characterization

3.1.1. SEM micrographs

The effect of acid activation on the adsorbent surfaces is reflected in the SEM micrographs – Figure 1(a) and 1(b). the ABC surface clearly has relatively larger particles than NBC, which appears to be compact with irregularly shaped particles. The micrographs of ABC show that acid treatment produced distinct spatial structures and dis-aggregation and reduced the size of the bentonite structure. Khalfa *et al.* (2016) found the same and suggested that acid activation improves the spatial structure of geo-sorbents.

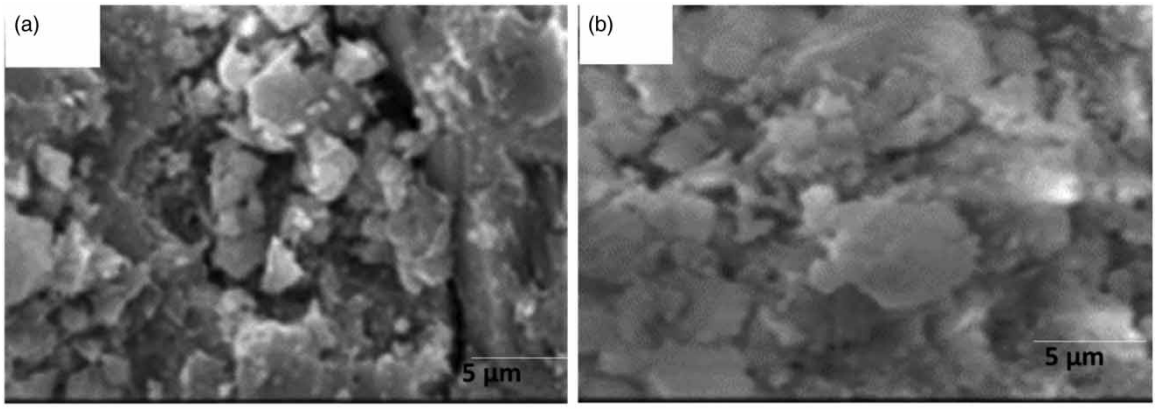

Figure 1 | SEM micrograph of (a) ABC and (b) NBC.

3.1.2. XRD patterns

The XRD results revealed considerable differences in the symmetry, sharpness, and position of the $d(001)$ plane diffraction peak (Figure 2(a) and 2(b)). The patterns from both NBC and ABC showed the presence of kaolinite, quartz, and montmorillonite, indicating that the smectite phase is present (Holmboe *et al.* 2012). As can be seen, the primary peaks for ABC shifted to smaller 2θ angles than those for NBC due to the increased interlayer

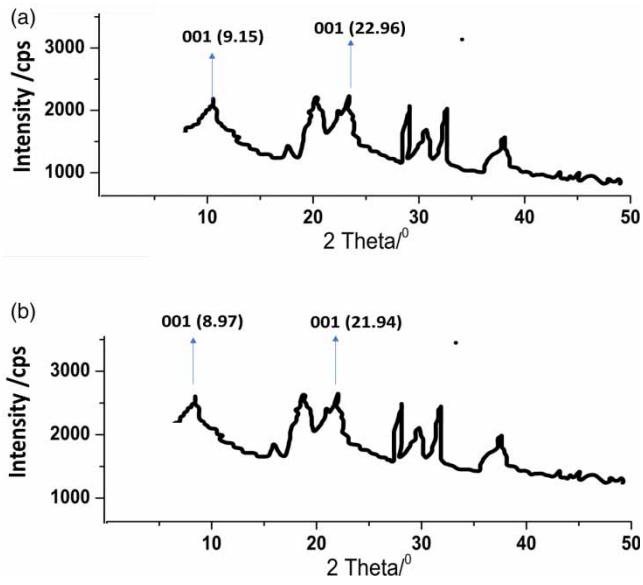

Figure 2 | XRD pattern of (a) ABC and (b) NBC.

distances. The ABC's basal spacing was reduced from 2.04A^0 ($2\theta = 9.15$) to 2.00A^0 ($2\theta = 8.97$), and both the octahedral and tetrahedral sites might have been altered.

3.1.3. FTIR spectra

The bands on the FTIR spectra for both NBC and ABC between 1,200 and 700 cm^{-1} could be attributed to silicates (Figure 3(a) and 3(b)). Those between 3,589 and 3,500 cm^{-1} could be attributed to structural hydroxyl groups and water molecules in the bentonite clay layers, as reported by Noyan *et al.* (2007).The bands at 3,446 cm^{-1} for NBC are assigned to the O–H stretching vibration of the clay's silanol (Si–OH) groups (coordinated to octahedral Al^{3+}cations) and HO–H vibration of the water molecules adsorbed on the bentonite surface, respectively, while that at 1,600 cm^{-1} reflects the angular deformation H–O–H bond of interlayer water molecules in the silicate matrix. The bands around 808 and 915 cm^{-1} are attributed to Al–Mg–OH and Al–Al–OH, respectively (Kumararaja *et al.* 2017).

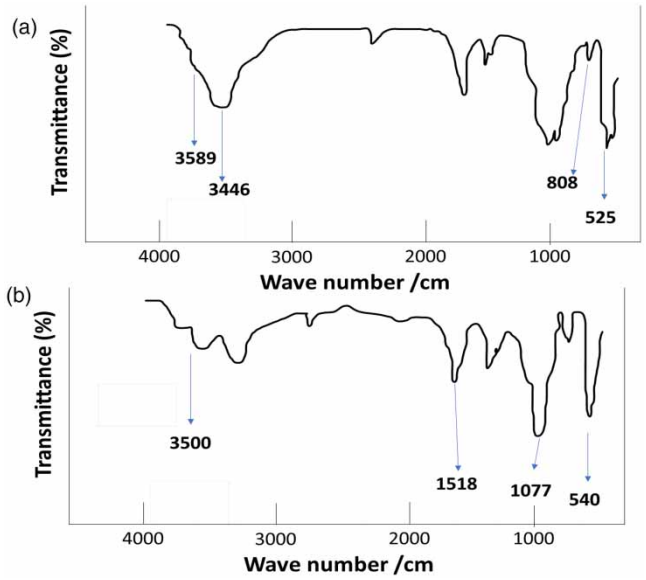

Figure 3 | FTIR spectra of (a) ABC and (b) NBC.

Activation of the clay led to penetration of the bentonite layers by the proton (H^+) from the acid (HNO_3), the penetrating proton becoming attached to the -OH group, resulting in partial dissolution and dihydroxylation of the smectite structure. The changes caused by the acid attack on the absorption bands are shown in Figure 3(b). The band around 3,500 cm^{-1} for ABC is characteristic of -OH stretching. However, acid attack reduced the OH stretching band intensities at 3,589 cm^{-1}. In general, there was no significant difference between the ABC and NBC FTIR bands. The only observed changes were minor wavenumber shifts and decreased band intensities. This indicated that the bentonite structure was not completely altered (Sdiri *et al.* 2014).

3.1.4. BET analysis

Figure 4 shows the nitrogen adsorption-desorption isotherms measured on NBC and ABC. Both samples show type IV adsorption isotherms and a large uptake is observed near saturation pressure.

The porosity was determined using conventional nitrogen isotherm analysis – Table 1. Both NBC and ABC are mesoporous, their pores having diameters within the range 2 to 50 nm. The adsorbent pores (D_p) of ABC were smaller than those of NBC, while the specific surface (S_{BET}) and total pore volume (V_T) of ABC were larger than those of NBC, as also reported by Eloussaief & Benzina (2010). Acid treatment opens the platelet edges, increasing the surface area and pore diameter.

3.2. Adsorption isotherm

Adsorption isotherms are mathematical expressions used to evaluate the distribution and interaction between sorbate and sorbents (Ololade *et al.* 2018). The Freundlich and Langmuir models (Equations (3) & (4), and (5)

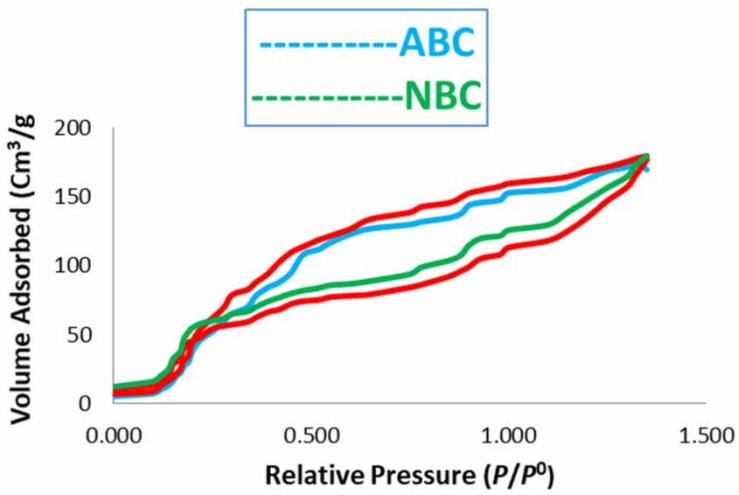

Figure 4 | N_2-sorption isotherms obtained from BET analysis.

Table 1 | Porous properties of NBC and ABC

Sample	S_{BET} (m^2/g)	V_{mic} (cm^3/g)	$V_{meso+mac}$ (cm^3/g)	V_T (cm^3/g)	D_p (nm)
NBC	46	0.04 (24%)	0.13 (76%)	0.17	14.78
ABC	76	0.05 (26%)	0.14 (74%)	0.19	10.00

& (6), respectively) were used to fit the experimental data obtained after equilibration. The magnitude of the regression correlation coefficient (R^2) reflects the quality of the isotherm fit to the experimental data.

$$Freundlich\ non-linear: \quad q_e = K_F\, C_e^N \tag{3}$$

$$Freundlich\ linear: \quad lnq_e = lnk_f + (1/n) lnC_e \tag{4}$$

$$Langmuir\ non-linear: q_e = \frac{q_{max} K_L C_e}{1 + K_L C_e} \tag{5}$$

$$Langmuir\ linear: \frac{C_e}{q_e} = \frac{1}{q_{max}} K_L + \frac{C_e}{q_{max}} \tag{6}$$

$$R_L = \frac{1}{1 + K_{Lq_{max}} C_0} \tag{7}$$

where N (dimensionless) and K_F (mg/g) $(L/mg)^N$) are the intensity parameter (a measure of site energy heterogeneity) and Freundlich constant; K_L (L/mg) and q_{max} (mg/g) the Langmuir constant (associated with solute–surface interaction energy) and maximum adsorption capacity, respectively; q_{max} (mg/g) the maximum adsorption capacity; C_e the liquid phase equilibrium concentration (mg/L), and q_e the solid-phase concentration (mg/g) (Ololade *et al.* 2018).

The model parameters for NBC and ABC are presented in Table 2, and Figure 5 display the plots for Langmuir and Freundlich for Fe^{2+}, Zn^{2+}, Ni^{2+} adsorption onto the two forms of bentonite. The Freundlich adsorption capacities, K_F, and intensity, K_L, are highest for ABC, suggesting that the tendency for multilayer adsorption is enhanced by acidified activation, which also improved the natural clay's surface morphology (Figure 1, Table 1). The value of 1/n, between 0.1 and 1, shows good adsorption, confirming the adsorbent's heterogeneity, and heterogeneous adsorption of Fe^{2+}, Zn^{2+}, Ni^{2+} on the surface of ABC.

The Langmuir model was efficient in analyzing adsorption data for all ions studied, but the Freundlich multilayer adsorption model best fit the experimental data, with higher R^2 values. The q_{max} values for ion binding onto the adsorbent decreased as $Fe^{2+} > Ni^{2+} > Zn^{2+}$, whereas K_L, which determines the sorption, showed that the

Table 2 | Summary of Freundlich and Langmuir sorption parameters for Fe^{2+}, Ni^{2+} and Zn^{2+} onto NBC and ABC

		NBC			ABC		
Model	**Parameter**	***Fe²⁺***	***Ni²⁺***	***Zn²⁺***	***Fe²⁺***	***Ni²⁺***	***Zn²⁺***
Freundlich	K_f	0.248	0.028	0.057	0.771	0.285	0.482
	N	6.01	2.99	4.00	9.47	6.46	7.19
	R^2	*0.979*	*0.973*	*0.971*	*0.982*	*0.995*	*0.988*
Langmuir	$q_{max\ (mg/g)}$	3.65	0.96	0.74	1.65	0.48	0.44
	$K_{L\ (L/mg)}$	0.60	0.55	0.42	0.86	0.78	0.67
	R^2	*0.968*	*0.943*	*0.961*	*0.971*	*0.963*	*0.964*

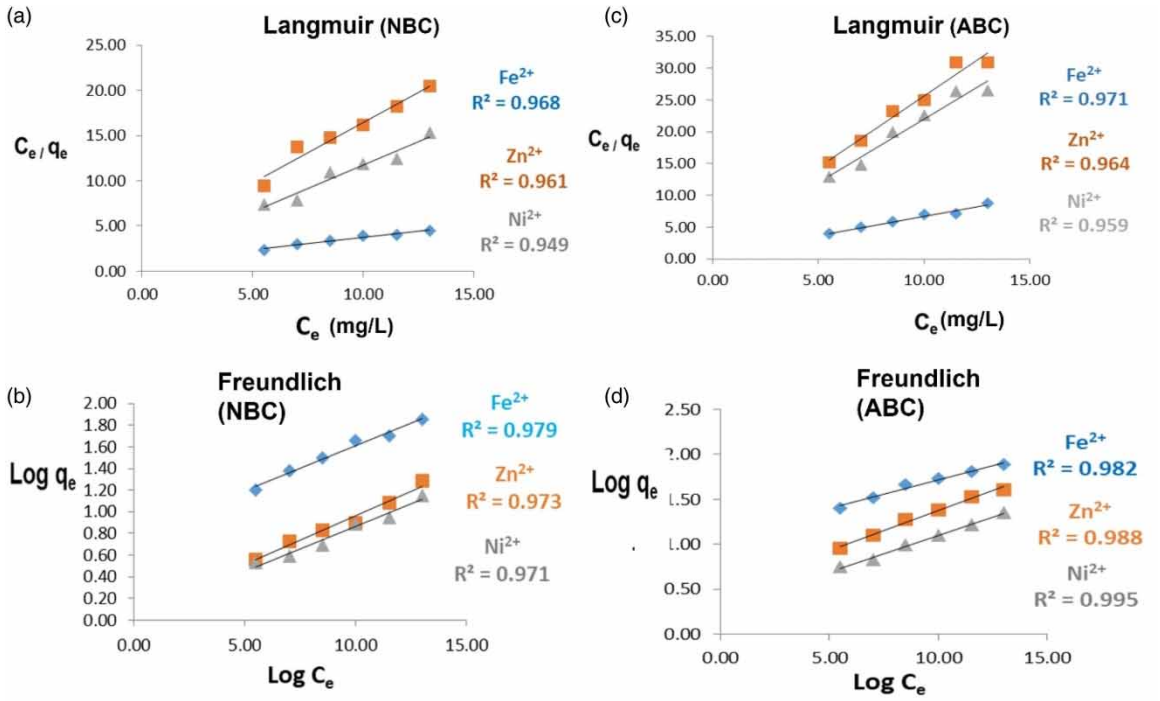

Figure 5 | Sorption isotherm plots for (a,b) NBC and (c,d) ABC for Fe^{2+}, Ni^{2+} and Zn^{2+}.

ABC sites had greater affinity for Fe^{2+}, Zn^{2+}, and Ni^{2+} than NBC, and they also decreased in the order $Fe^{2+} > Ni^{2+} > Zn^{2+}$. This is due to the ions' varying electronegativity, which affects the surface ion exchange potential (Igberase *et al.* 2017).

The electronegativities of Fe, Ni and Zn on the Pauling scale are 1.83, 1.80, and 1.60, respectively, which agrees with the adsorption capacity and affinity of the metal ions to NBC and ABC. Since the K_L values for these ions are higher for ABC than NBC, this indicates more favorable adsorption for the ions using ABC, which is similar to what Igberase *et al.* (2017) reported for Pb, Zn, Cu, Ni, and Cd adsorption by modified ligand in a single batch experiment.

3.3. Adsorption kinetics

The pseudo-first-order, pseudo-second-order and intraparticle diffusion kinetic models (Equations (8)–(11)) were compared in order to establish the mechanism and rates of the adsorption process (Ololade *et al.* 2018; Zhao *et al.* 2020).

$$q_t = q_e(1 - e^{-K_1 t}) \tag{8}$$

$$q_t = \frac{q_e^2 K_2 t}{q_e K_2 t + 1} \tag{9}$$

$$\frac{t}{q_t} = \frac{1}{k_2 q_e^2} + \frac{1}{q_e} t \tag{10}$$

$$q_t = K_{id} t^{0.5} + C \tag{11}$$

where q_e and q_t (mg/g) are the amount of adsorbate sorbed per mass of adsorbent at equilibrium and at time (t), respectively; K_1 (1/min) and K_2 (1/mg/g × min) pseudo-first-order and pseudo-second-order rate constants, respectively; and K_{id} (mg/g × $min^{1/2}$) and C (mg/g) the intraparticle diffusion rate constant.

The kinetic parameters from the models are summarized in Table 3 and the kinetic plots displayed in Figure 6. The pseudo-second-order model best fit the kinetic data, with R^2 values exceeding 0.99 for both NBC and ABC adsorption, but K_2 and K_{id} suggest that adsorption by NBC is faster.

Table 3 | Sorption kinetics coefficients for heavy metal adsorption by NBC and ABC

		NBC			ABC		
Kinetic model	**Parameter**	Fe^{2+}	Ni^{2+}	Zn^{2+}	Fe^{2+}	Ni^{2+}	Zn^{2+}
Pseudo-first-order	$q_{e\ (exp)}$	13.80	2.00	1.65	13.80	2.00	1.65
	$q_{e\ (mg/g)}$	5.83	1.45	0.59	4.64	1.22	0.48
	$K_{1\ (min^{-1})}$	0 .036	0.057	0.051	0.056	0.045	0.062
	R^2	*0.564*	*0.632*	*0.700*	*0.675*	*0.788*	*0.813*
Pseudo-second-order	$q_{e\ (mg/g)}$	13.92	2.13	1.70	13.84	2.05	1.67
	$K_{2\ (g/mg/min)}$	0.004	0.279	0.303	0.003	0.119	0.171
	R^2	*0.992*	*0.994*	*0.996*	*0.995*	*0.997*	*0.999*
Intraparticle diffusion	$K_{id\ (mg/gmin^{1/2})}$	14.305	2.357	1.724	11.252	1.986	1.593
	R^2	*0 .999*	*0.975*	*0.989*	*0.931*	*0.971*	*0.990*

Table 3 shows that the experimental q_e values are close to the calculated values in NBC and ABC for the pseudo-second-order model. This further confirms that the second-order kinetic pathway is correct and suggests that ion-exchange/chemisorption may have occurred (Yu *et al.* 2015). The R^2 values for the intraparticle diffusion model suggest that diffusion occurred for both NBC and ABC adsorption. A significant number of the heavy metal ions may have diffused into the adsorbents' pores before being adsorbed.

3.4. Adsorption thermodynamics

The thermodynamics of Fe^{2+}, Zn^{2+}, and Ni^{2+} ion adsorption was conducted using Van't Hoff plot – Equations (12) and (13) – for different temperatures.

$$\ln Kd = \frac{\Delta S^\circ}{R} - \frac{\Delta H^\circ}{RT} \tag{12}$$

$$\Delta G^\circ = -RTln\,Kd \tag{13}$$

where T is the thermodynamic temperature (K), R the gas constant (8.314 J/mol K), ΔS the change in entropy (J/mol.K), ΔH the change in enthalpy (kJ/mol), and ΔG the change in the Gibbs free energy (kJ/mol).

The plots of ln K_d versus 1/T for the adsorption of Fe^{2+}, Zn^{2+}, Ni^{2+} is presented in Figure 7. The related results given in Table 4 show that the adsorption is endothermic and spontaneous, with positive and negative values of enthalpy and Gibb's free energy, respectively. For all three heavy metals, both adsorption spontaneity and driving force are greater onto ABC than NBC as the temperature increases. A similar finding was reported by Igberase *et al.* (2017). With increasing temperature, the Gibbs energy magnitude decreases in conformity with the adsorption process' endothermic nature, as an increased energy supply would lead to enhanced adsorption. The enthalpy change (ΔH^o) sign associated with sorption will consist of (1) enthalpy change for dehydration (ΔH^o_d), which can be expected to be positive because energy is necessary to break the ion–water and water–water bonding of the hydrated metal ions, and (2) enthalpy change for complexing ($\Delta H^o_{c)}$, which will make ΔH^o more

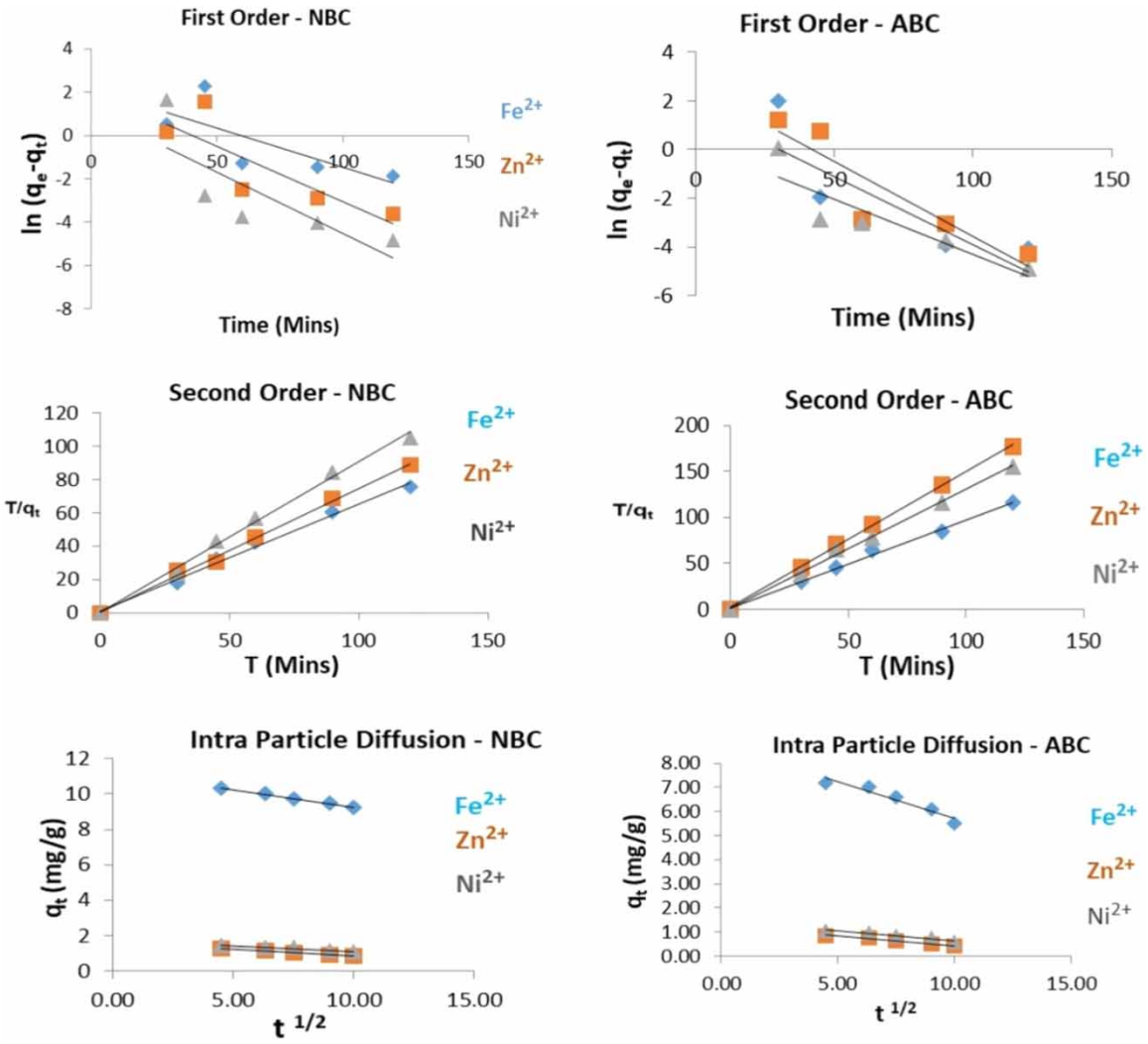

Figure 6 | First-order, second-order and intraparticle diffusion model plots for NBC and ABC.

negative because of metal complex formation (Ding *et al.* 2012). The positive ΔH^o value obtained for Fe^{2+}, Zn^{2+}, and Ni^{2+} adsorption shows that dehydration may be more significant than complexation in the system. The enthalpy changes for adsorption were less than 40 kJ/mol for ABC and NBC, indicating that sorption for the ions studied was controlled by a physical mechanism (Ding *et al.* 2012). The higher positive entropy change ($\Delta S°$) values for adsorption onto ABC is due to some structural changes of the activated adsorbent. The degree of randomness increased at the solid-liquid interface in ABC than NBC. This has been attributed to a physical adsorption process, and favors complexation and stable interaction (Yang *et al.* 2010).

Thermodynamic data on metal adsorption on clays are limited, with less still Fe^{2+}, Zn^{2+}, and Ni^{2+} adsorption onto bentonite, and none on acid-activated bentonite. Yavuz *et al.* (2003) found that ΔH^o, ΔS^o and ΔG^o for Cu^{2+} adsorption onto Turkish kaolinite are 39.5 kJ/mol, 11.7 J/mol.K and −4.6 kJ/mol, respectively. Echeverria *et al.* (2003) found that ΔH^o, ΔS^o and ΔG^o for Ni^{2+} adsorption onto illite have values of +16.8 J/mol, 58 J/mol.K and −1.04 kJ/mol. ΔH^o, ΔS^o and ΔG^o for Cu^{2+} adsorption on surfactant-modified montmorillonite were reported as 7.05 kJ/mol, 9.09 J/mol.K and − 9.66 kJ/mol, respectively, by Lin & Juang (2002).

3.5. Effects of contact time, pH and oxidation using hydrogen peroxide

Figure 8(a) shows the results of wastewater treatment using different equilibration times (30, 45, 60, 90, and 120 minutes). After equilibration with a 5 g bed of either NBC or ABC, the supernatant was analyzed. As can be seen, uptake of the ions studied was quicker with ABC than NBC, likely due to variation in sorption affinities (K_L). The rate of ion uptake from the effluent was also found to increase with increasing contact time, as reported by Murithi *et al.* (2012). It is believed that the decrease in mass transfer coefficient (K_{id}) of the diffusion-regulated

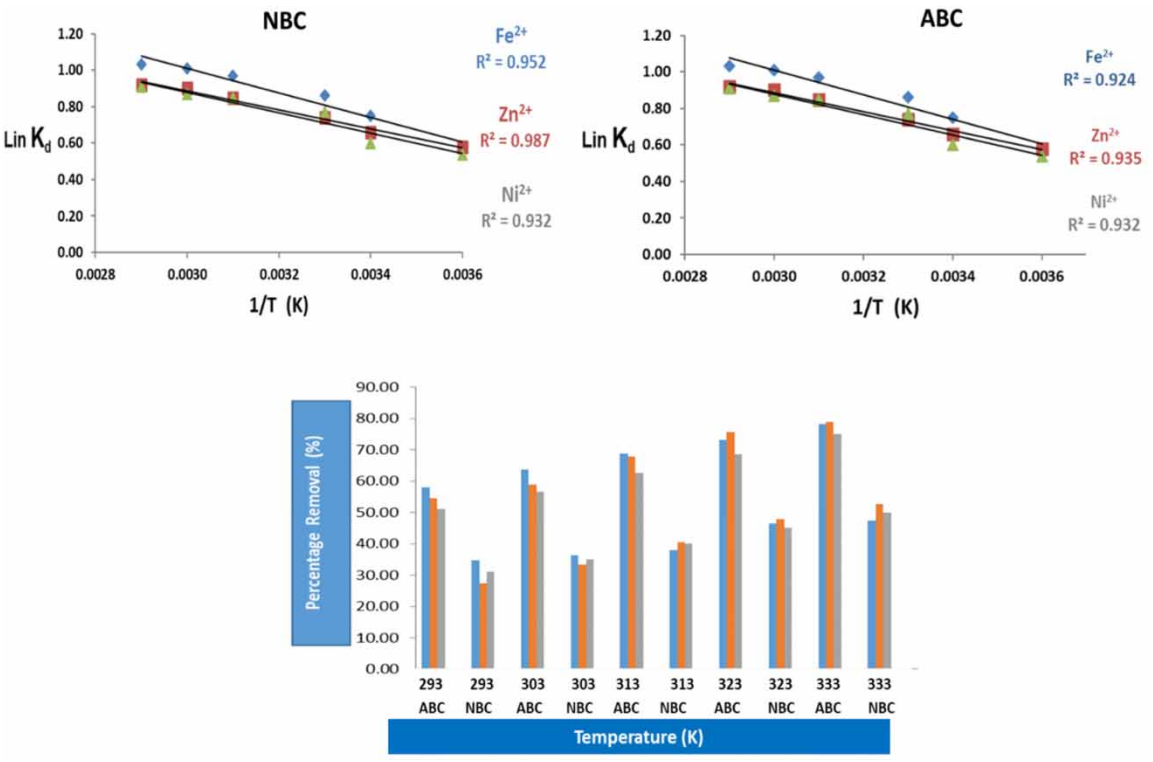

Figure 7 | Van't Hoff plots for Fe^{2+}, Zn^{2+} and Ni^{2+} adsorption onto NBC and ABC at 293, 303, 313, 323 and 333 K.

Table 4 | Thermodynamic parameters for metal ion adsorption onto NBC and ABC

		NBC			ABC		
Parameter		***Fe²⁺***	***Ni²⁺***	***Zn²⁺***	***Fe²⁺***	***Ni²⁺***	***Zn²⁺***
ΔH^o (kJ/mol)		5.59	4.63	4.30	0.77	0.29	0.48
ΔS^o (J/mol.K)		25.16	21.23	20.30	9.47	6.46	7.19
ΔG^o (kJ/mol)	*273 K*	− 1.27	−1.14	− 1.23	− 3.04	− 2.34	− 2.34
	293 K	− 1.77	−1.57	−1.63	−3.38	−2.84	−3.08
	303 K	− 2.03	−1.78	−1.84	−3.87	−3.09	−3.47
	313 K	− 2.28	−1.99	− 2.04	− 4.36	− 3.35	− 3.86
	323 K	− 2.53	−2.21	− 2.24	− 4.85	− 3.60	− 4.25
	333 K	− 2.78	−2.42	− 2.45	− 5.34	− 3.85	− 4.64

metal ion/adsorbent reaction was largely responsible for the enhanced removal efficiency (Bhattacharya *et al.* 2006). Increases in the amount of active sites, porosity and surface area on the ABC, after acid treatment, are responsible for the higher ion removal from the wastewater. For ABC, there was a reduction in Zn^{2+} concentration from 1.65 to 0.42 mg/L (74.5% removal), Ni^{2+} removal was from 2.00 to 0.60 mg/L (70.0% removal), and Fe^{2+} from 13.80 to 5.50 mg/L (60.1%). On the other hand, removal by NBC, starting from the same initial concentrations as ABC, reported Zn^{2+}, Ni^{2+}, Fe^{2+} final concentrations of 0.83 mg/L (49.7% removal), 1.07 mg/L (46.5%), and 9.25 mg/L (33.0%), respectively.

pH influences the adsorption chemistry of many aqueous pollutants, and particularly the adsorbent surface characteristics and metal ion speciation (Attahirua *et al.* 2012). Figure 8(b) clearly shows the effects of varying the pH (pH 4, 6, 8, 10, and 12) on heavy metal ion removal, while keeping other conditions constant. Sorption sites are prone to protonation or deprotonation depending on the solution pH, while the adsorbent surface can also be positively or negatively charged under differing pH conditions (Ololade *et al.* 2018). At pH 4, when the adsorbent is positively charged, low uptake is observed for the ions studied, for both ABC and NBC. Like charges repel. Furthermore, H^+ competes with metal ions in acidic pH. However, as the pH increases, more Fe^{2+}, Zn^{2+},

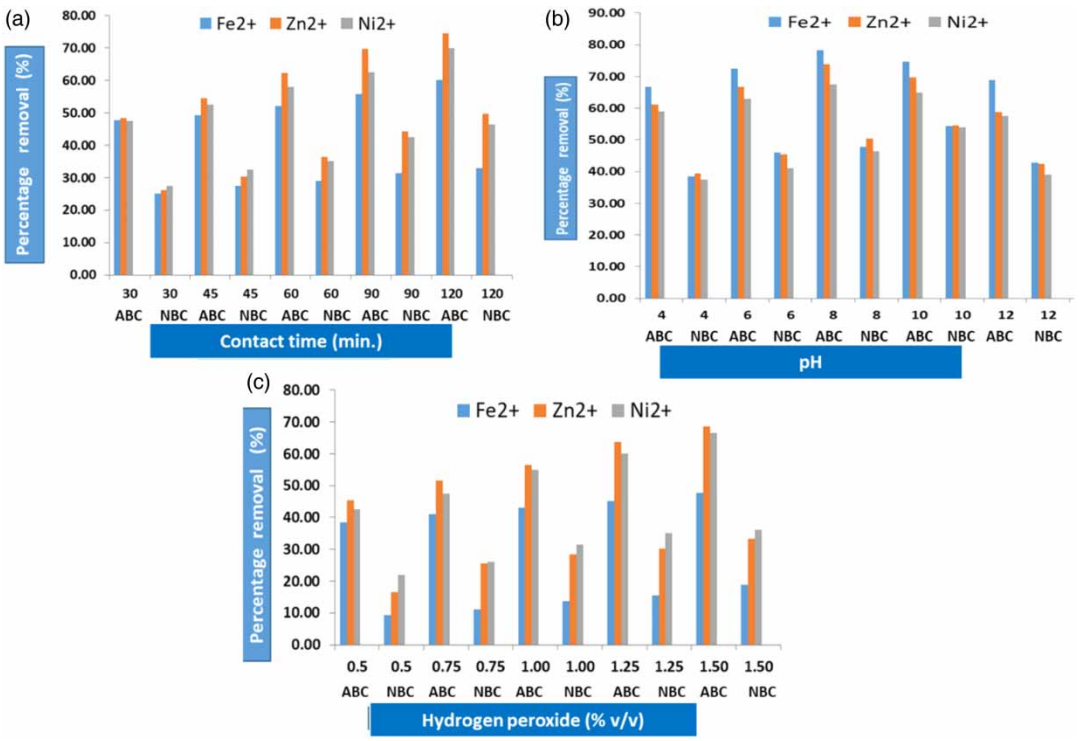

Figure 8 | Influence of process variables on the removal efficiencies of NBC and ABC: (a) contact time, (b) solution pH (c) oxidation using hydrogen peroxide.

and Ni^{2+} are adsorbed, because they exist as $FeOH^{+}$, $ZnOH^{+}$ and $NiOH^{+}$, and the sorbent is deprotonated at basic pH (Ibigbami *et al.* 2016).

The results show that, as the wastewater pH increases in the presence of ABC and NBC, the amounts of the heavy metals adsorbed increase due to electrostatic attraction. However, the removal efficiency of Fe^{2+}, Zn^{2+}, Ni^{2+} by ABC is higher than that of NBC, due to its greater surface area and sorption site availability (cavities and/or pores).

Analysis of the treatment results showed that the optimum proportional removal efficiencies occurred at pH 8 for ABC and pH 10 for NBC. In ABC, adsorption capacities are in the order $Fe^{2+} >>> Zn^{2+} >>> Ni^{2+}$. Iron is precipitated, complexed, or adsorbed easily because Fe^{2+} is oxidized to Fe^{3+} and precipitates as $Fe(OH)_3$. On the contrary, the adsorption trend onto NBC follows the order, $Zn^{2+} >>> Fe^{2+} >>> Ni^{2+}$ ions, which may be attributed to the smaller ionic size of Zn^{2+} compared to Fe^{2+} and Ni^{2+} (Izidoro *et al.* 2013).

Figure 8(c) shows the result of varying the H_2O_2 dose (0.5 to 1.50 v/v%) on heavy metal removal, at 30-minute contact time and using 5 g of NBC or ABC. H_2O_2 acts an oxidizing agent for heavy metal ions. Peroxide application enhanced the treatment efficiency for the metal ions studied for both adsorbents, possibly due to ionic interaction between the oxidized metals and adsorbents. However, ABC showed more ionic interaction than NBC for all of the metals studied. The formation of hydrophobic/insoluble metal hydroxides like Zn(OH), Ni(OH, Fe(OH) enhances partitioning of the metal pollutants onto the adsorbents' hydrophobic surfaces (Pignatello *et al.* 1999; Kinuthia *et al.* 2020).

3.6. Comparison with previous studies

Many minerals and plant materials have been used to remove metals from polluted water (Önal & Sarikaya 2007; Bhatnagar *et al.* 2010; Internò *et al.* 2015). Adsorption of metal ions using clay minerals such as: palygorskite from Dwaalboom, South Africa for Pb^{2+}, Ni^{2+}, Cr^{3+}, Cu^{2+} at pH 7 (Potgieter *et al.* 2006); montmorillonite from India's Karnataka region for Cu^{2+} at pH 2.5 (Oubagaranadin & Murthy 2010); montmorillonite and kaolinite for Fe^{2+}, Co^{2+}, and Ni^{2+} at pH 5.7 (Bhattacharyya & Gupta 2008); Ca-bentonite from Almeria, Spain, and an Na-exchanged bentonite from Milos, Greece, for Cr^{3+} (pH 4), Ni^{2+} (pH 6), Zn^{2+} (pH 6), Cu^{2+} (pH 5) and Cd^{2+} (pH 6) (Alvarez-Ayuso & Garćia-Sánchez 2003); kaolinite from China's Longyan region for Pb^{2+} (pH 6), Cu^{2+} (pH 6.5), Cd^{2+} (pH 7) and Ni^{2+} (pH 7) (Jiang *et al.* 2010); palygorskite for Pb^{2+} at pH 5 (Fan *et al.* 2009), illite

from Tunisia for Pb^{2+} at pH 7 (Eloussaief & Benzina 2010); smectite from Tunisia for Pb^{2+} at pH 4 (Chaari *et al.* 2008); illite from Tunisia for Cd^{2+} and Cr^{3+} at pH 3.5 (Ghorbel-Abid *et al.* 2010). Although, all of the above are geo-sorbents, they exhibit different heavy metal removal efficiencies due to their differing physicochemical properties. The degree of alteration of the active surface and clay structure porosity produced by acids depends, among other things, on the clay's chemical composition and interlayer cation types, the acid applied, and its concentration, temperature and time of action (Bhattacharyya & Gupta 2008).

4. CONCLUSIONS

The adsorption of Fe^{2+}, Zn^{2+}, Ni^{2+} from a pharmaceutical effluent was investigated using NBC and ABC. Bentonite is an efficient adsorbent due to its high specific surface and pore volume, negatively charged surface and other physicochemical properties, as found in this study.

In this study, bentonite was activated successfully using nitric acid, as shown by FTIR, CEC, SEM, XRD, and BET studies. It was shown that ABC offered maximum proportional removals of about 89.9, 81.8 and 75.5% for Zn^{2+}, Fe^{2+} and Ni^{2+}, while NBC's removal capacities were 63.9, 59.6 and 58.7% for the same species. The results indicate that heavy metal removal by bentonite was affected considerably by process conditions, such as solution pH, contact time, and temperature, and can be enhanced by oxidation using hydrogen peroxide.

The experimental data were fitted to various kinetic models, which revealed that the pseudo-second-order model fit best, while it appears that diffusion plays a role in the process. It can be concluded that film and intraparticle diffusion occurred simultaneously during adsorption process considering the strong correlation coefficients (Table 3).

Adsorption isotherm models such as those derived by Langmuir and Freundlich were used to describe the experimental adsorption data, and plots showed that Freundlich's multilayer adsorption model fit best, with better R^2 values, showing good adsorption and confirming the adsorbent's heterogeneity. The results show that adsorption was controlled mainly by electrostatic attraction and/or ion exchange. The thermodynamic parameters (ΔH^o, ΔS^o and ΔG^o) for Fe^{2+}, Ni^{2+}, Zn^{2+} adsorption show that the process behaves endothermically for both ABC and NBC. ABC's ΔH^o value exceeds that of NBC, indicating that Fe^{2+}, Zn^{2+} and Ni^{2+} are held more strongly by ABC, their magnitude shows moderately stronger bonds between ABC and Fe^{2+}, Zn^{2+}ions than Ni^{2+}. The negative value of ΔG for the ions studied on both ABC and NBC shows the spontaneous and favorable nature of adsorption at various temperatures. ΔG^o becomes increasingly negative with increasing temperature, suggesting that adsorption is more favorable.

The study confirmed that modifying bentonite using nitric acid enhanced its specific surface. Finally, it has been shown that ABC, with its improved specific surface compared to NBC, can remove pollutants effectively (especially heavy metals) from pharmaceutical wastewater.

ACKNOWLEDGEMENTS

The authors are grateful to the Federal Institute of Industrial Research (FIIRO), Oshodi, Lagos State, Nigeria for the supply of bentonite clay.

CONFLICT OF INTEREST

The authors declare that they have no conflict of interest.

DATA AVAILABILITY STATEMENT

All relevant data are included in the paper or its Supplementary Information.

REFERENCES

Abu-Danso, E., Peräniemi, S., Leiviskä, T., Kim, T., Tripathi, K. M. & Bhatnagar, A. 2020 Synthesis of clay-cellulose biocomposite for the removal of toxic metal ions from aqueous medium. *Journal of Hazardous Materials* **381**, 120871. https://doi.org/10.1016/j.jhazmat.2019.120871.

Adebiyi, F. M., Ore, O. T., Adeola, A. O., Durodola, S. S., Akeremale, O. F., Olubodun, K. O. & Akeremale, O. K. 2021 Occurrence and remediation of naturally occurring radioactive materials in Nigeria: a review. *Environmental Chemistry Letters* **19**, 3243–3262. https://doi.org/10.1007/s10311-021-01237-4.

Ahmetović, M., Šestan, I., Begić, S., Tučić, E. & Hasanbašić, A. 2019 Biosorption of heavy metals from the multi-component systems of the galvanic industry using brewer's grain as adsorbents. *International Journal of Applied Science* **5**(5), 26–32.

Alvarez-Ayuso, E. & Garćia-Sánchez, A. 2003 Removal of heavy metals from waste waters by natural and Na-exchanged bentonites. *Clays and Clay Minerals* **51**(5), 475–480.

Attahirua, S., Shiundua, P. M. & Wambu, E. W. 2012 Removal of Cr (III) from aqueous solutions using a micaceous polymineral from Kenya. *International Journal of Physical Sciences* **7**(8), 1198–1204.

Bergaya, F. & Vayer, M. 1997 CEC of clays: measurement by adsorption of a copper ethylenediamine complex. *Applied Clay Science* **12**(3), 275–280.

Bhatnagar, A., Vilar, V. J., Botelho, C. M. & Boaventura, R. A. 2010 Coconut-based biosorbents for water treatment – a review of the recent literature. *Advances in Colloid and Interface Science* **160**(1–2), 1–15.

Bhattacharya, A. K., Mandal, S. N. & Das, S. K. 2006 Adsorption of Zn (II) from aqueous solution by using different adsorbents. *Chemical Engineering Journal* **123**(1–2), 43–51.

Bhattacharyya, K. G. & Gupta, S. S. 2008 Adsorption of a few heavy metals on natural and modified kaolinite and montmorillonite: a review. *Advances in Colloid and Interface Science* **140**(2), 114–131.

Burakov, A. E., Galunin, E. V., Burakova, I. V., Kucherova, A. E., Agarwal, S., Tkachev, A. G. & Gupta, V. K. 2018 Adsorption of heavy metals on conventional and nanostructured materials for wastewater treatment purposes: a review. *Ecotoxicology and Environmental Safety* **148**, 702–712.

Chaari, I., Fakhfakh, E., Chakroun, S., Bouzid, J., Boujelben, N., Feki, M., Rocha, F. & Jamoussi, F. 2008 Lead removal from aqueous solutions by a Tunisian smectitic clay. *Journal of Hazardous Materials* **156**(1–3), 545–551.

Ding, L., Deng, H., Wu, C. & Han, X. 2012 Affecting factors, equilibrium, kinetics and thermodynamics of bromide removal from aqueous solutions by MIEX resin. *Chemical Engineering Journal* **181**, 360–370.

Echeverrıa, J., Indurain, J., Churio, E. & Garrido, J. 2003 Simultaneous effect of pH, temperature, ionic strength, and initial concentration on the retention of Ni on illite. *Colloids and Surfaces A: Physicochemical and Engineering Aspects* **218**(1–3), 175–187.

Eloussaief, M. & Benzina, M. 2010 Efficiency of natural and acid-activated clays in the removal of Pb (II) from aqueous solutions. *Journal of Hazardous Materials* **178**(1–3), 753–757.

Fan, Q., Li, Z., Zhao, H., Jia, Z., Xu, J. & Wu, W. 2009 Adsorption of Pb (II) on palygorskite from aqueous solution: effects of pH, ionic strength and temperature. *Applied Clay Science* **45**(3), 111–116.

Ghorbel-Abid, I., Galai, K. & Trabelsi-Ayadi, M. 2010 Retention of chromium (III) and cadmium (II) from aqueous solution by illitic clay as a low-cost adsorbent. *Desalination* **256**(1–3), 190–195.

Holmboe, M., Wold, S. & Jonsson, M. 2012 Porosity investigation of compacted bentonite using XRD profile modeling. *Journal of Contaminant Hydrology* **128**(1–4), 19–32. https://doi.org/10.1016/j.jconhyd.2011.10.005.

Ibigbami, T. B., Dawodu, F. A. & Akinyeye, O. J. 2016 Removal of heavy metals from pharmaceutical industrial wastewater effluent by combination of adsorption and chemical precipitation methods. *American Journal of Applied Chemistry* **4**(1), 24–32.

Igberase, E., Osifo, P. & Ofomaja, A. 2017 The adsorption of Pb, Zn, Cu, Ni, and Cd by modified ligand in a single component aqueous solution: equilibrium, kinetic, thermodynamic, and desorption studies. *International Journal of Analytical Chemistry*. https://doi.org/10.1155/2017/6150209.

Internò, G., Lenti, V. & Fidelibus, C. 2015 Laboratory experiments on diffusion and sorption of heavy metals in a marine clay. *Environmental Earth Sciences* **73**(8), 4443–4449.

Ismadji, S., Soetaredjo, F. E. & Ayucitra, A. 2015 Modification of Clay Minerals for Adsorption Purpose. In: *Clay Materials for Environmental Remediation* (Ismadji, S., Soetaredjo, F. E. & Ayucitra, A. eds.). Springer International Publishing, Cham, pp. 39–56.

Izidoro, J. D. C., Fungaro, D. A., Abbott, J. E. & Wang, S. 2013 Synthesis of zeolites X and A from fly ashes for cadmium and zinc removal from aqueous solutions in single and binary ion systems. *Fuel* **103**, 827–834.

Jiang, M. Q., Jin, X. Y., Lu, X. Q. & Chen, Z. L. 2010 Adsorption of Pb (II), Cd (II), Ni (II) and Cu (II) onto natural kaolinite clay. *Desalination* **252**(1–3), 33–39.

Kanamarlapudi, S. L. R. K., Chintalpudi, V. K. & Muddada, S. 2018 Application of biosorption for removal of heavy metals from wastewater. *Biosorption* **18**, 69.

Khalfa, L., Cervera, M. L., Bagane, M. & Souissi-Najar, S. 2016 Modeling of equilibrium isotherms and kinetic studies of Cr (VI) adsorption into natural and acid-activated clays. *Arabian Journal of Geosciences* **9**(1), 1–14.

Kinuthia, G. K., Ngure, V., Beti, D., Lugalia, R., Wangila, A. & Kamau, L. 2020 Levels of heavy metals in wastewater and soil samples from open drainage channels in Nairobi, Kenya: community health implication. *Scientific Reports* **10**(1), 1–13. https://doi.org/10.1038/s41598-020-65359-5.

Kumararaja, P., Manjaiah, K. M., Datta, S. C. & Sarkar, B. 2017 Remediation of metal contaminated soil by aluminium pillared bentonite: synthesis, characterisation, equilibrium study and plant growth experiment. *Applied Clay Science* **137**, 115–122. https://doi.org/10.1016/J.CLAY.2016.12.017.

Lin, S. H. & Juang, R. S. 2002 Heavy metal removal from water by sorption using surfactant-modified montmorillonite. *Journal of Hazardous Materials* **92**(3), 315–326.

Maged, A., Iqbal, J., Kharbish, S., Ismael, I. S. & Bhatnagar, A. 2020 Tuning tetracycline removal from aqueous solution onto activated 2:1 layered clay mineral: characterization, sorption and mechanistic studies. *Journal of Hazardous Materials* **384**, 121320. https://doi.org/10.1016/j.jhazmat.2019.121320.

Murithi, G., Onindo, C. O. & Muthakia, G. K. 2012 Kinetic and equilibrium study for the sorption of Pb (II) ions from aqueous phase by water hyacinth (*Eichhornia crassipes*). *Bulletin of the Chemical Society of Ethiopia* **26**(2), 181–193.

Noyan, H., Önal, M. & Sarıkaya, Y. 2007 The effect of sulphuric acid activation on the crystallinity, surface area, porosity, surface acidity, and bleaching power of a bentonite. *Food Chemistry* **105**(1), 156–163. https://doi.org/10.1016/j.foodchem.2007.03.060.

Ololade, I. A., Adeola, A. O., Oladoja, N. A., Ololade, O. O., Nwaolisa, S. U., Alabi, A. B. & Ogungbe, I. V. 2018 In-situ modification of soil organic matter towards adsorption and desorption of phenol and its chlorinated derivatives. *Journal of Environmental Chemical Engineering* **6**(2), 3485–3494. https://doi.org/10.1016/j.jece.2018.05.034.

Önal, M. & Sarıkaya, Y. 2007 Preparation and characterization of acid-activated bentonite powders. *Powder Technology* **172**(1), 14–18.

Ore, O. T. & Adeola, A. O. 2021 Toxic metals in oil sands: review of human health implications, environmental impact, and potential remediation using membrane-based approach. *Energy, Ecology and Environment* **6**(2), 81–91. https://doi.org/10.1007/s40974-020-00196-w.

Oubagaranadin, J. U. K. & Murthy, Z. V. P. 2010 Isotherm modeling and batch adsorber design for the adsorption of Cu (II) on a clay containing montmorillonite. *Applied Clay Science* **50**(3), 409–413.

Pignatello, J. J., Liu, D. & Huston, P. 1999 Evidence for an additional oxidant in the photoassisted Fenton reaction. *Environmental Science & Technology* **33**(11), 1832–1839. doi:10.1021/es980969b.

Potgieter, J. H., Potgieter-Vermaak, S. S. & Kalibantonga, P. D. 2006 Heavy metals removal from solution by palygorskite clay. *Minerals Engineering* **19**(5), 463–470.

Sdiri, A. T., Higashi, T. & Jamoussi, F. 2014 Adsorption of copper and zinc onto natural clay in single and binary systems. *International Journal of Environmental Science and Technology* **11**(4), 1081–1092.

Uddin, M. K. 2017 A review on the adsorption of heavy metals by clay minerals, with special focus on the past decade. *Chemical Engineering Journal* **308**, 438–462. https://doi.org/10.1016/j.cej.2016.09.029.

Yang, S., Zhao, D., Zhang, H., Lu, S., Chen, L. & Yu, X. 2010 Impact of environmental conditions on the sorption behavior of Pb (II) in Na-bentonite suspensions. *Journal of Hazardous Materials* **183**(1–3), 632–640.

Yavuz, Ö., Altunkaynak, Y. & Güzel, F. 2003 Removal of copper, nickel, cobalt and manganese from aqueous solution by kaolinite. *Water Research* **37**(4), 948–952.

Yu, F., Ma, J. & Bi, D. 2015 Enhanced adsorptive removal of selected pharmaceutical antibiotics from aqueous solution by activated graphene. *Environmental Science and Pollution Research* **22**(6), 4715–4724. doi:10.1007/s11356-014-3723-9.

Zhao, C., Ma, J., Li, Z., Xia, H., Liu, H. & Yang, Y. 2020 Highly enhanced adsorption performance of tetracycline antibiotics on KOH-activated biochar derived from reed plants. *RSC Advances* **10**(9), 5066–5076.

First received 1 December 2021; accepted in revised form 10 February 2022. Available online 22 February 2022